Journal of Clinical Monitoring and Computing
https://doi.org/10.1007/s10877-020-00553-4

ORIGINAL RESEARCH

Quantitative assessment of consciousness during anesthesia without EEG data

Clément Dubost[1,2] · Pierre Humbert[2] · Laurent Oudre[2,3] · Christophe Labourdette[2] · Nicolas Vayatis[2] · Pierre-Paul Vidal[2,4]

Received: 13 June 2019 / Accepted: 29 June 2020

Abstract
Assessing the depth of anesthesia (DoA) is a daily challenge for anesthesiologists. The best assessment of the depth of anesthesia is commonly thought to be the one made by the doctor in charge of the patient. This evaluation is based on the integration of several parameters including epidemiological, pharmacological and physiological data. By developing a protocol to record synchronously all these parameters we aim at having this evaluation made by an algorithm. Our hypothesis was that the standard parameters recorded during anesthesia (without EEG) could provide a good insight into the consciousness level of the patient. We developed a complete solution for high-resolution longitudinal follow-up of patients during anesthesia. A Hidden Markov Model (HMM) was trained on the database in order to predict and assess states based on four physiological variables that were adjusted to the consciousness level: Heart Rate (HR), Mean Blood Pressure (MeanBP) Respiratory Rate (RR), and AA Inspiratory Concentration (AAFi) all without using EEG recordings. Patients undergoing general anesthesia for hernial inguinal repair were included after informed consent. The algorithm was tested on 30 patients. The percentage of error to identify the actual state among Awake, LOC, Anesthesia, ROC and Emergence was 18%. This protocol constitutes the very first step on the way towards a multimodal approach of anesthesia. The fact that our first classifier already demonstrated a good predictability is very encouraging for the future. Indeed, this first model was merely a proof of concept to encourage research ways in the field of machine learning and anesthesia.

Keywords Anesthesia · Depth of anesthesia · Data base · Machine learning · Prediction

1 Introduction

The three commonly admitted goals of anesthesia are lack of experience of surgery, nociceptive blockade and immobility for the needs of surgery [1]. Depth of Anesthesia (DoA) has been defined by experts as "the probability of non-response to stimulation, calibrated against the strength of the stimulus, the difficulty of suppressing the response, and the drug-induced probability of non-responsiveness at defined effect site concentrations" [2]. When consciousness does not disappear totally, the patient may be aware of the intervention and keep memories of the surgery. This condition, named "intraoperative awareness with explicit recall", however rare, may cause post-operative stress disorder [3].

In that context, the gold-standard to quantify brain activity, during anesthesia, remains the electroencephalogram (EEG). Hence, several monitoring systems using EEG-based index have been proposed for DoA assessment, but they all have limitations [4]. Besides, no point-of-care gold standard monitoring prevails for the DoA. The most used index is the Bispectral Index, (BIS, Covidien, Boulder, CO) proposed in the 2000s by an American company as a measure of the effect of anesthetics on the brain [5, 6]. The Bispectral Index provides a numerical value from 0 to 100 (no cerebral activity to awake and responsive) allowing for more accurate tailoring of the anesthetics administered. The usual numerical value for a surgical anesthesia lies between 40 and 60, whereas values < 40 indicate over-dosage of anesthetics and

✉ Clément Dubost
clement.dubost@hotmail.fr

1 Begin Military Hospital, Saint-Mandé, France

2 Université Paris-Saclay, ENS Paris-Saclay, CNRS, Centre Borelli, 91190 Gif-sur-Yvette, France

3 L2TI, Université Paris 13, Villetaneuse, France

4 Institute of Information and Control, Hangzhou Dianzi University, Zhejiang, China

Published online: 13 July 2020

values > 80 lack of anesthetics. Despite being largely used, mostly in the US, DoA's monitor presents several drawbacks such as high inter-individual variability [7], low performance with volatile anesthetics [8], long latency and interferences with surgical knife, artifacts from movements or from forced air warming therapy [9]. Another EEG-based index is the Sample-entropy introduced by Richman et al. [10]. It is a variant of the approximate entropy that gives information on the complexity of a time series such as an EEG signal. Altogether then, although the EEG remains to these days the gold standard for the evaluation of the DoA it has some limitations and it is time consuming. Additional sensors would be useful. This may explain why, in routine clinical context, the best evaluation of the DoA is often deemed to be the one completed by the anesthesiologist. Therefore, a DoA monitor should ideally provide an evaluation without the help of the EEG signal.

Compulsory monitoring during the anesthesia includes heart rate, blood pressure, respiratory and muscle function, but it does not include the main target of the anesthetics i.e. the brain [11]. To date, only a few teams aimed at evaluating the DoA using multiple parameters analysis. In 2014, Schneider et al. developed the Anesthesia Multimodal Index of Consciousness (AMIC) [12]. Their model included demographic data from the patients, the nature and quantity of the drugs injected and standard physiological signals such as heart rate, mean arterial blood pressure and EEG signals (Approximate entropy or Weighted spectral median frequency). It demonstrated a significantly better predictive value of the DoA compared to BIS values. In this study, the sampling rates for analysis of the physiological signals ranged between 10 s to 5 min. Their results are promising but we believe that increasing the sampling rate is critical in order to develop a real time approach. More recently, two studies have shown that artificial neuron networks fed with several standard parameters recorded during anesthesia could assess the DoA [13, 14]. Sadrawi et al. used values sampled every 5-s on average (0.2 Hz), for both the EEG data and the physiologic parameters. In 2012, Liu et al. developed the University of Queensland Vital Signs Dataset [15], aimed at recording continuous monitoring values during anesthesia. Their recording was limited to 10 min, which does not allow proper recording of anesthesia procedures. Finally, databases have been used for a long time in anesthesiology but mainly to assess risks [16] and improve safety in anesthesia practices [17].

In the present study, we have tried to combine these different approaches. First, we continuously recorded at high frequency the physiologic parameters routinely monitored during anesthesia, including a 2-channel EEG in order to build a database of properly labeled variables. Then using a machine learning approach, we successfully used that database to create an algorithm aimed at determining the DoA without relying on EEG data.

2 Methods

2.1 Participants

The study was conducted in the Begin military teaching hospital, Saint-Mandé, France. The study has been approved by Pr. JE BAZIN, head of the institutional ethical review board of the French society of anesthesiology (SFAR) under the number IRB 00010254-2016–2018. The patient criteria of inclusions were: 18 years of age minimum, inguinal hernia repair under general anesthesia, acceptance of the patient with low comorbidity score (patient classified ASA 1 or 2) and written informed consent given by the patient.

2.2 Anesthesia protocol

All patients were pre-oxygenated via face-mask by 100% oxygen for at least 3 min before induction. SUFENTANIL 0.3 µg/kg was injected rapidly followed, 3 min later, by 2–4 mg/kg of PROPOFOL in combination with KETAMINE 20 mg. When required for the surgery, patients were paralyzed following induction with a bolus of 0.17 mg/kg of CISATRACURIUM. After tracheal intubation, patients were ventilated with tidal volume of 6 mg/kg ideal-body weight, 5 cmH_2O Positive end-expiratory Pressure (Peep) and a respiratory rate between 10 and 14 to maintain $EtCO_2$ between 30 and 40 mmHg. Anesthesia was maintained with SEVOFLURANE MAC age-adjusted (e.g. 1.0). Dose adjustments were made by the anesthesiologist in charge of the patient depending on clinical variables available. Once asleep, patients received a transversus abdominis plane block with single bolus dose of ROPIVACAÏNE 150 mg.

2.3 Equipments

2.3.1 Hardware

Personal computer: Any of the three classics OS: Windows, Macintosh and Linux were accepted.

Monitoring device: In the Begin military teaching hospital, each room in the intensive care unit or in the operating theatre is equipped with a multi parametric monitoring device called a scope and more precisely a Carescape monitor B850, from General Electrics (GE) Healthcare™ Finland Oy, Helsinki, Finland. The common monitoring includes Electrocardiogram (EKG), Arterial Pulse Oxymetry (SpO_2), Non-invasive or Invasive Arterial Blood Pressure. Optional monitoring offers more possibilities, such as gas analysis, EEG, plethysmography, BIS or Entropy.

These variables can be monitored separately and displayed on a touch-screen monitor in real time.

2.3.2 Software

VSCapture: In 2013, John Georges Karippacheril published a letter presenting the open-source VSCapture software [18], a C# program available in SourceForge, an online Web-based service. After a slight modification, this software was used to record and save all the data presented in Table 1 at the specified sampling frequencies imposed by the sensors specificities. Importantly, all the recorded variables were synchronized within the GE scope, which allowed for a precise correlation between the different parameters.

Python and Matlab™: Libraries for preprocessing and signal analysis were: for Python—numpy, scipy, matplotlib. for Matlab™—Signal Processing Toolbox.

Table 1 Variables in the acquisition classified by modules

Variables	Units	abbreviation
EKG—300 Hz		EKG
Electrocardiogram 1	V	
E-EEG module—100 Hz		EEG
Electroencephalogram 1 2	V	
Basics module—1 Hz		HR
Heart rate	/min	
Systolic arterial blood pressure	mmHg	SBP
Diastolic arterial blood pressure	mmHg	DBP
Mean arterial blood pressure	mmHg	MBP
Saturated percentage of dioxygen	/100%	SpO_2
Gas analysis module—1 Hz		Et CO_2
End tidal carbon dioxide	mmHg	
Anesthesia agent		AA
AA expiratory concentration	/100%	AA Et
AA inspiratory concentration	/100%	AA Fi
Total minimum alveolar concentration	/100%	AA MAC SUM
Fraction inspired of dioxygen	/m	Fi O_2
Mean alveolar concentration	/m	MAC
Fraction inspired nitrous oxide	/m	Fi N_2
End tidal nitrous oxide	/m	Et N_2O
Respiratory rate	/min	RR
BIS module—1 Hz		BIS
Bispectral index		
BIS burst suppression ratio	%	BIS BSR
BIS electromyography	dB	BIS EMG
BIS signal quality index	%	BIS SQI

2.4 Measurements

In order to perform multimodal analysis, the EKG and all the physiological variables routinely followed up for anesthesia (Table 1) were included in the recording. EEG was added to characterize objectively the state of consciousness [19, 20].

2.4.1 Electroencephalogram (EEG)

EEG signal is the reference measurement for the monitoring of brain electrical activity [21–24]. We used a 2-channel EEG recorded at 100 Hz using the optional module E-EEG sold by GE™. Channels F4-A1 and C4-A1 were selected because of their ease of installation and their appropriate position on the scalp for anesthesia assessment (Fig. 1). Indeed, several studies have demonstrated sustained modifications in the anterior part of the brain under general anesthesia [25, 26]. During a classical intervention involving sevoflurane, the frequencies of interest are below 30 Hz [27]. For this reason, the sampling rate of the EEG–100 Hz—was considered suitable for the present study.

2.4.2 Electrocardiogram (EKG)

The EKG provides a continuous and real time representation of the electrical activity of the heart due to variations of the myocyte cells potential. The technical specifications of the device allow recording all EKG channel at 300 Hz. Monitoring the heart's electrical activity during general anesthesia is a legal requirement and it is recommended by the American Society of Anesthesiologists® (ASA).

2.4.3 Physiological variables

Physiological variables were recorded at 1 Hz in their respective unit. During a general anesthesia for a low-risk patient, the 22 variables presented in Table 1, were chosen as they included all the monitoring recommended by the ASA for anesthesia practice. Other variables were also recorded,

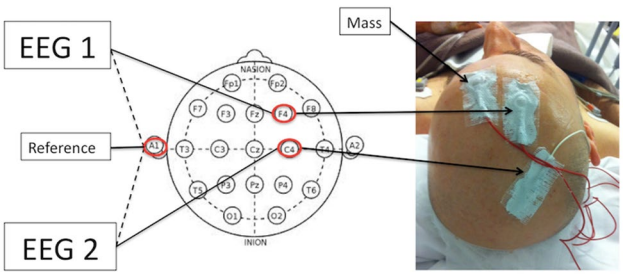

Fig. 1 EEG montage with standard reference and mass positions. EEG 1 thus corresponds to F4-A1 and EEG 2 to C4-A1

such as ST-segment measurement, temperature and entropy. They are presented in Table 1.

2.5 Stepwise procedure

2.5.1 Materials needed

2.5.1.1 GE™ Carescape monitor B850 Different modules added to the GE™ Carescape monitor to record the desirable variables as presented in Table 1.

Four dry electrodes—two for the EEG recording, one for the mass and one for reference—connected to the EEG module.

One computer with the VSCapture software installed. Note that because of C# architecture, the software can run on all OS (Linux, Windows or Macintosh).

2.5.2 Sensors installation

For EEG recording, the scalp of each patient was cleaned with an abrasive cleaning fluid (Reegaponce pasta®; MEI, Toulon, France); low-impedance electrode pasta (Grass EC2 electrode cream®; Astro-Med, Warwick, Rhode Island, USA) was placed under a re-usable Capsulex electrode (Micromed Spa®, Mogliano Veneto, Italy). Electrodes impedance was kept under 2 kohm to ensure a proper EEG recording with minimal noise. The placement of the four electrodes are illustrated in Fig. 1.

2.5.3 Connectivity

The four usb ports of the GE™ Carescape monitor B850 are USB 2.0 ports. The computer was connected to the scope via a VGA/USB cable plugged on the monitor's second or third usb port. The first usb port is often used for the tactile keyboard and therefore should be avoided. The fourth usb port should also be avoided because its data transfer rate is smaller than for the three others.

2.5.4 Acquisition

Once VSCapture was started and the appropriate usb port was selected, recordings began automatically. Four.csv files were created: one for each EEG channel, one for the EKG channel and one for all the physiological variables. Another file, named "AS3Rawoutput1.raw" was automatically created but had no specific utility for our purpose and was deleted at the end of the recording. The first column of data displayed the time sampling and the other columns displayed the values of the recorded variables. All the files were collected in a folder called "Data", which was created at each launch.

2.6 Identification of the brain state without EEG data

2.6.1 Hidden Markov model (Fig. 2)

Formally, a (finite-state) Markov chain is a tuple (S, T, π) where S is a finite set of states, T is the transition matrix such as $T(s, \dot{s}) = P\left(S_{t+1} = s \vee S_t = \dot{s}\right)$ and π is the initial distribution. The main property of a Markov chain can be expressed as *"The future is independent of the past given the present"*. In mathematical term, $P\left(S_{t+1} = \dot{s} \vee S_t\right) = P\left(S_{t+1} = \dot{s} \vee S_t, ..., S_0\right)$. Thus, a HMM is a more complex Markov chain where states $S_t \in S$ cannot be directly observed. However, the model is supposed to provide observations carrying information about the states. Observations $O_i \in O$ give an assumption on those hidden states via a distribution $P\left(S_i \vee O_i\right)$ which is the probability of a state S_i given a particular observation O_i. For instance, the probability to be in state Anesthesia if we observe all the variables equals to 0. Hence, a HMM is a tuple (S, T, O, B, π) where B is a stochastic matrix such as $B(s, x) = P\left(O_i = x \vee S_i = s\right)$. Observations were encoded with thresholds obtained by the calculation of the percentiles. This operation discretized the observations to construct

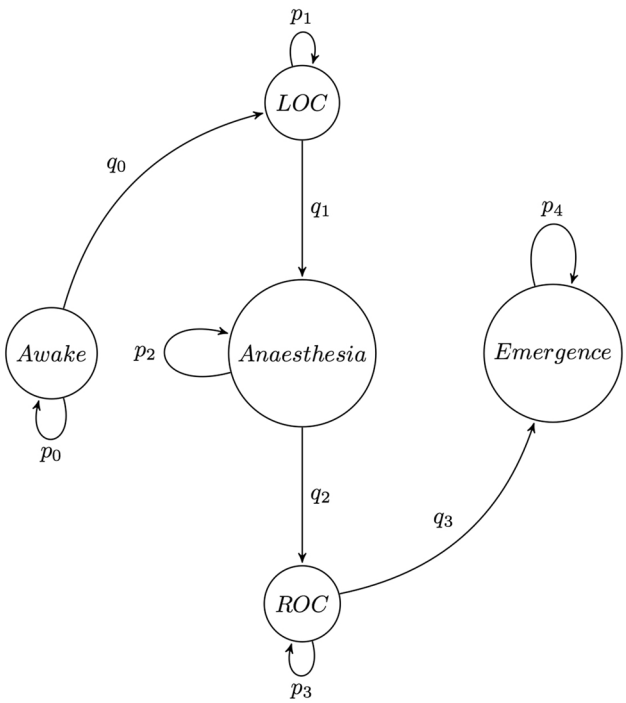

Fig. 2 Diagram of the HMM process. The 5 stages of the consciousness are represented. LOC and ROC are respectivley "Loss Of Conscioueness" and "Recovery of Conciouness". At each stage i there is a probability pi to stay in this stage or qi to go in another one. The HMM model assess the values of (pi)i to predict the most probable sequence of stages of a patient during the surgery

the Belief matrix B. To improve the model given in [28] an additional preprocessing was necessary for optimal results. As each patient was unique, thresholds values needed to be personalized. A low value for a patient could be a high value for another patient. Note that, a tradeoff is necessary between the refinement of the model and the accuracy of the estimate probability. Indeed if the set of observations O is large, learning the probabilities is undermined.

2.6.2 EEG validation

EEG has been widely studied and several tools are validated for its interpretation during anesthesia. In the signal processing landscape, Fourier theory is one of the most popular tools. Another one is the Wavelet theory. It is used for epilepsy detection [29], EEG classification [30] and can help quantifying brain activity [31]. Temporal Series and auto-regressive processes could also provide solutions for an approximation of the frequency domain [32].

EEG analysis should be performed by using appropriated mathematical tools based on time–frequency decomposition (Fig. 3). This implies recognizing actual waves, which are presented in Table 2.

Before any transformations and frequencies extraction of the signal we filtered it with a Butterworth bandpass filter of order 5 between 1 and 20 Hz. This filtering removed the potential drift below 1 Hz, to keep the frequencies characterizing GA and to remove any noise over 20 Hz.

The spectrogram representation is certainly the easiest and fastest way to analyze an EEG and to present the data. Indeed, it is common to use it to visualize the variations in time and frequency of a signal. For instance, let s be a signal, sampled at frequency rate f_s and composed of N samples. Let $s[n]$ be the value of s at sample $n \in [\![0, N-1]\!]$.

Table 2 Definitions of waves with their names and frequencies

Waves	Frequencies (Hz)
δ- Delta	0–4
θ- Thêta	4–8
α- Alpha	8–14
β- Bêta	>14

Literature brings several frequency intervals definition for waves. We are presenting the most commonly accepted values for the different waves

Given a window size N_w, and a hop size N_h, we denote by $s^{(i)}$ the sub-signal of length N_w and starting at sample iN_h, i.e.

$$s^{(i)} = s\left[iN_h : iN_h + N_w - 1\right],$$

The spectrogram representation is based on the calculation of the squared Discrete Fourier Transform (DFT) on the overlapping sub-signals $s^{(i)}$. It can be represented as a matrix with coefficients equal to

$$spectro\{s\}[i,k] = \left|\sum_{n=0}^{N_w-1} w[n]s^{(i)}[n]e^{-2i\pi kn}\right|$$

where i is the frame number, k is the frequency bin associated with physical frequency $f = \frac{k}{N_w} f_s$ and w is a window of length N_w. This computation requires the choice of one window w, a window length N_w and a hop size N_h.

In the spectrogram produced in Fig. 4, each stage is easy to characterize. A classical window function called Hanning window or Hann window has been chosen. The window length N_w was set to $2^{10}/100 = 10.24$ s and the overlap to $N_h = N_w/2 = 5.12$ s.

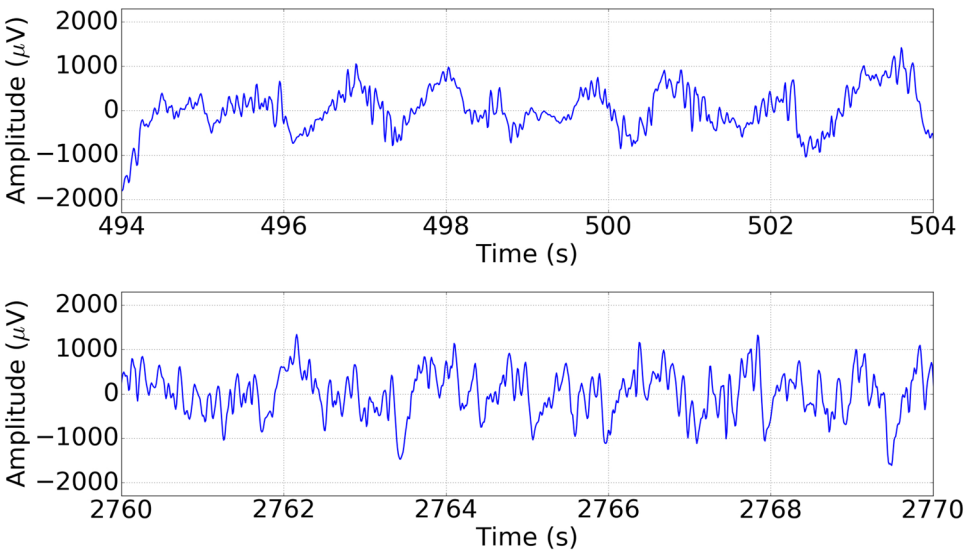

Fig. 3 EEG signal of a patient during two different periods of time. On top, the signal corresponds to an Awake patient while below, it represents a signal during an Anesthesia state

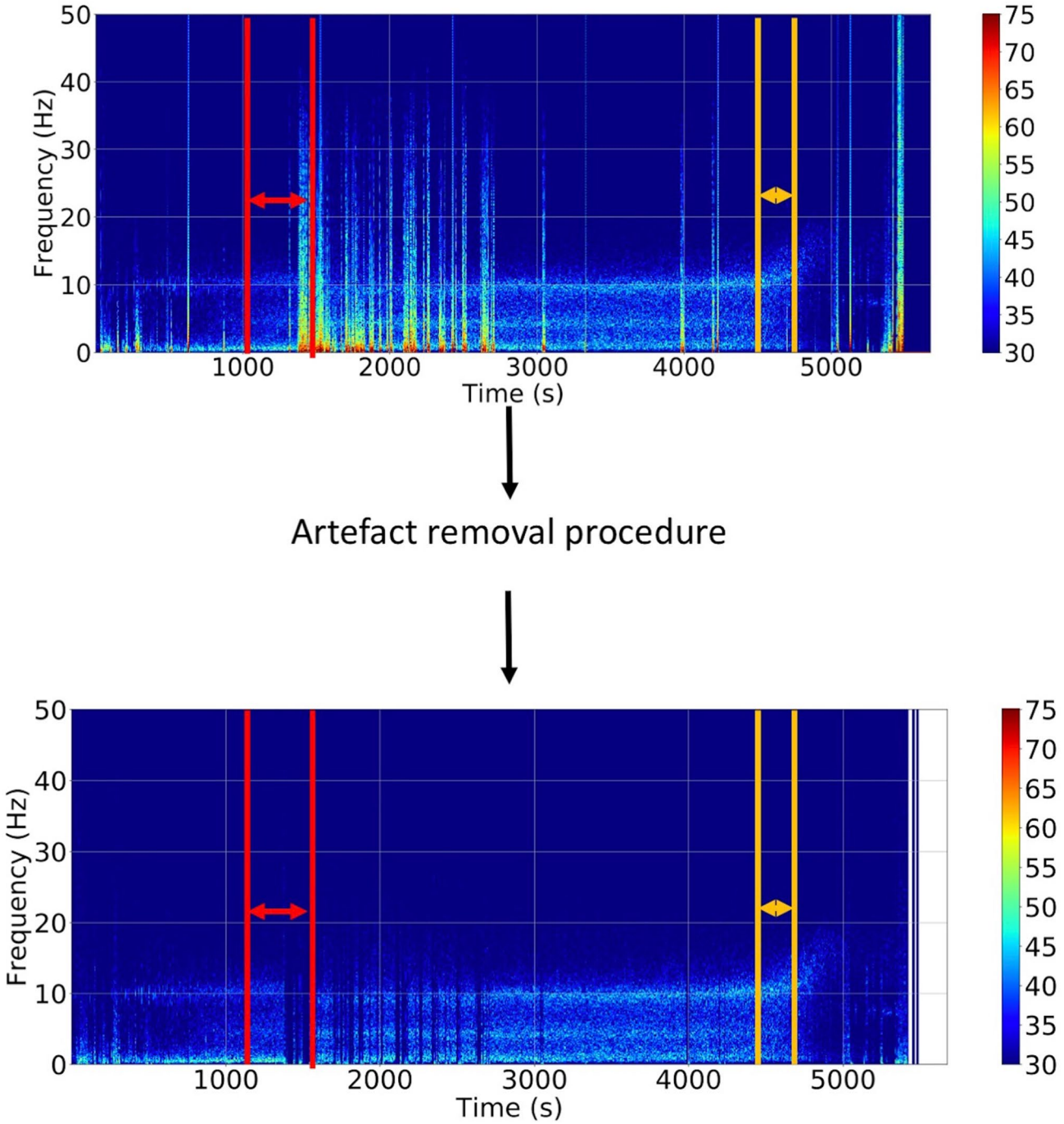

Fig. 4 Upper part: Raw spectrogram of a patient before an artifact removal procedure. Interferences resulted from a saturation of the measuring tools. Lower part: Typical spectrogram under sevoflurane after arteact removal procedure. Units are seconds (s) for the time, Hertz (Hz) for the frequencies. The Loss of Consciousness (LOC) stage is delimited by the red lines and the Recovery of Consciousness (ROC) stage by the orange ones

The result of the analysis is a sequence, which defined in time three states during the surgery: the Loss of Consciousness (LOC), the anesthesia and the Recovery of Consciousness (ROC). It allows supervised learning and supervised exploration for a better understanding of each stage.

3 Results

From February to May 2017, 43 patients have been included. The demographic data of the patients are presented in Table 3. Only patients with a high-quality EEG recording

Table 3 Demographic description of the population

Measures	Values
Age (year)	60 (24, 92)
Sex F/M	10/20
Weight (kg)	82 (50, 105)
Height (cm)	176 (159, 191)
ASA I/II	12/18

The values presented are medians (minimums, maximums)

(less than 10% of time with artefacts) were included in the algorithm.

3.1 Identification of depth of anesthesia through brain activities

In our case, the EEG was used as a groundtruth, to objectively confirm the brain states and compare them with the predictions. Below are detailed the analysis of the spectrograms that allow precise definition of the brain state throughout the intervention.

Figure 3 displays the EEG signal of a patient during two different periods of time. On top, the signal corresponds to an Awake patient while below, it represents a signal during an Anesthesia state. This example underlines the fact that identifying the state of anesthesia on the raw EEG signal is very challenging if not impossible.

Figure 5 displays the typical recording of an unremarkable general anesthesia for inguinal hernial repair. Under, the BIS curve was plotted to facilitate the analysis. Power values of interest varies from approximatively 35 to 60 dB. As expected, frequencies of interest are under 20 Hz and Band Frequencies are clearly identifiable in the Figure. A visual analysis allows an extraction of the different stages over time. The LOC, referring to the transition from awake to anesthesia, starts at the beginning of the α wave and ends at the beginning of the θ wave (between the red lines). Conversely, the ROC started with the disappearance of the θ wave and finishes when the α band is no longer identifiable (between white lines). The accurate and objective identification of the DoA was possible thanks to the determination of the waves on the spectrogram. The most important parameter are delays of transition which reflect the time for the different compartments of the brain to get into or out of deep

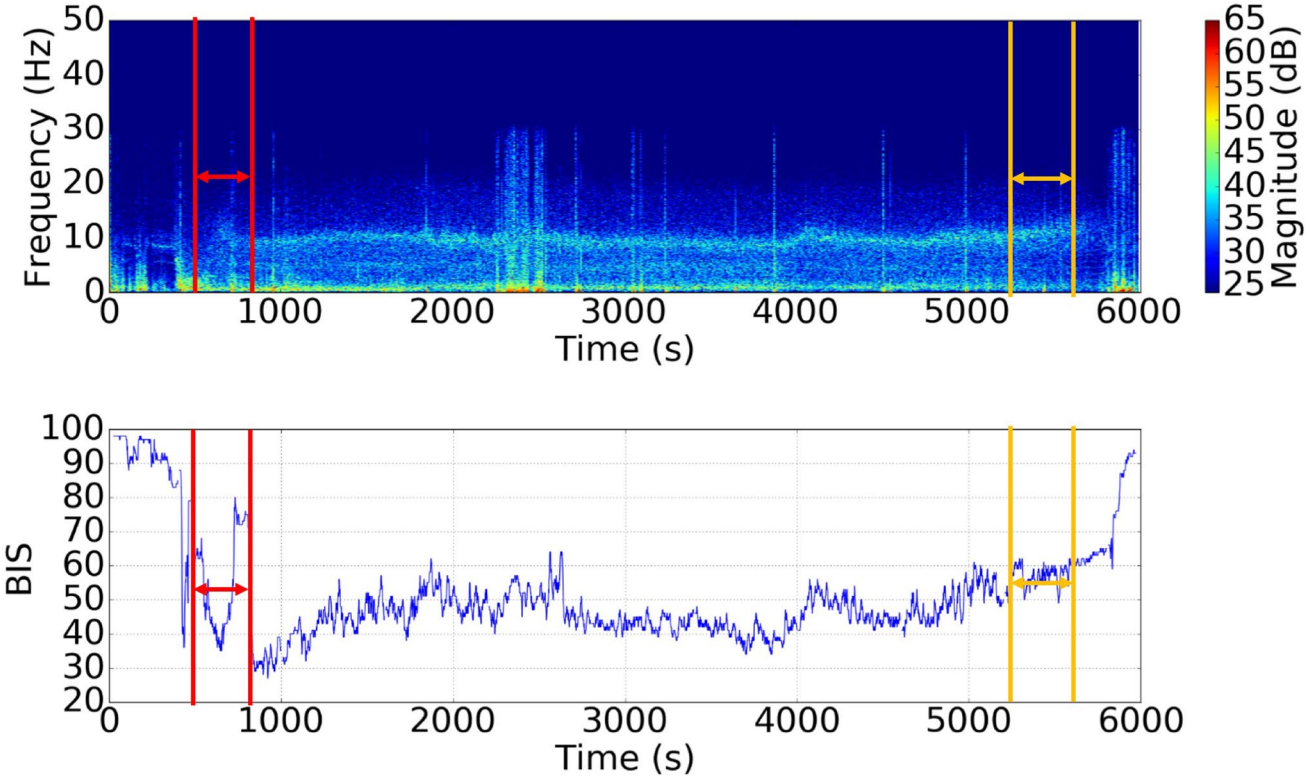

Fig. 5 On top, typical spectrogram during an anesthesia maintained by sevoflurane. Units are second (s) for time, Hertz (Hz) for frequency. The power in each band was then logarithmically transformed so that all spectral power was expressed in decibel (dB). Under, BIS curve during anesthesia of the same patient. The Loss of Consciousness (LOC) stage is delimited by the red lines and the Recovery of Consciousness (ROC) stage by the orange ones

anesthesia. It should be noticed that such clear spectrograms are possible because EEG was recorded with dedicated EEG electrodes and not extracted from the BIS sensors. This is not trivial as many researches are being performed with values derived from BIS sensor with a lower quality of signal. Figures 3 and 4 show two different ways of analyzing an EEG during an anesthesia for a single patient. In Fig. 3, the upper part presents the raw EEG of an awake patient, contrary to the lower part where the patient is asleep. A precise discrimination between the two states would have been hard if based only on those signals. Nevertheless, the absolute value of the amplitude of the signal during the awake stage is lower than during the anesthesia stage.

It is instructive to compare the BIS curve with our data. They often confirm the diagnosis of the stage determined by the EEG recordings. But sometimes, the BIS values are not well correlated with the stage of consciousness of the patient. It is the case at ' 900 s where values of the BIS became inexplicably high (Fig. 5). Transitions stages LOC and ROC were detected by the BIS with a consequent delay—1 min in our case. More precisely, the estimated probability of good detection of LOC before this delay is less than a 50/50 chance and is equals to 0:455 [33].

3.2 Identification of anesthesia state with physiological variables

3.2.1 Individual discretization process

Each observation consisted of quadruplets HR, MBP, RR, AAEt discretized using 3 thresholds and taking their values in the set {0, 1, 2, 3} - where 0 represents low values, and 3 high values. The discretization was calculated using Ckmeans, a clustering algorithm based on K-means which has been proven to outperform it in the one-dimensional case [34].

We made an exception for AAEt, which was discretized according to common anesthetic heuristics (i.e. with thresholds between 1 and 3%). The purpose of this calibration procedure was (1) to reduce the inter-patient variability while keeping the intra-patient variability by mapping similar physiological states into the same discretized state—a key part of the problem, as incoherent discretization led to contradictory events, (2) to train a model that automatically adapts to the demographic characteristics of patients (e.g. age, height, weight, BMI). An example of discretization is displayed in the Fig. 6.

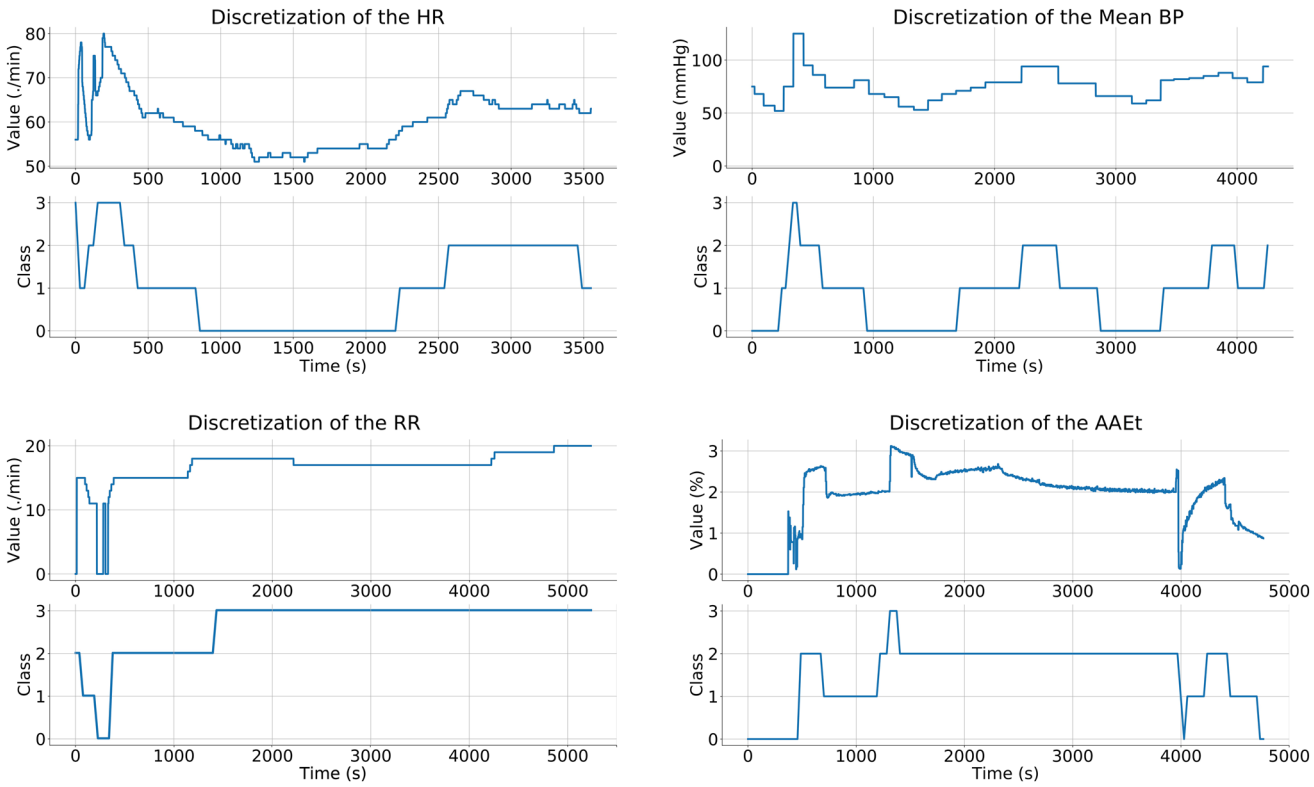

Fig. 6 Example of a discretization on the four variables, HR, MBP, RR and AAEt. For each variable, on the top the raw signal recorded by the monitor during the GA. On the bottom, its discretization in four classes via CKmean

3.2.2 Confusion matrix

We evaluated the performance of our algorithm using a confusion matrix. Each row of this matrix represents the predicted class while each column represents the true class. Hence, the value in the row i column j is the number of points predict in class i while they are actually in class j. The Fig. 7 panel A presents the matrix of confusion with the four variables included. The colour ranges from white (low value) to dark blue (high value). We can see that, even if the algorithm failed to predict the true class, its errors are mostly made on close classes. To emphasize that the model is not based only on the variable AAEt, this variable has been removed from the model and the confusion matrix is reevaluated (Fig. 7 panel B). We see that even without the AAEt variable, the model is able to return accurate predictions.

3.2.3 Performance of the algorithm

To assess the performance of the algorithm, we randomly separated the dataset in train and test sets. We progressively increased the number of patients in the train set and assessed its performance on patients of the test set. We observed that the performance stopped to improve after the inclusion of 20 patients.

Figure 8 displayed the prediction of the model for one patient. The important information of this figure is the delay required to anticipate a change of state. One possibility to evaluate this model and its capacity to predict states on new patients is to use a leave-one-out technique. For each evaluation, one patient is put aside and the tuple of the HMM is learned on the others. The error of prediction is calculated on this single patient. Finally, the global error amounts to the average of all the previously computed errors. We used this algorithm on 30 patients under general anesthesia for inguinal hernial repair [35]. The goal was to objectively identify the actual state among Awake, LOC, Anesthesia, ROC and Emergence. Each variable was divided as discussed above. The percentage of error for the prediction was 18%. The good performance obtained by our algorithm should be interpreted cautiously as only 30 patients were analyzed in this preliminary work.

3.3 Electrocardiogram segmentation: automatic QRS complex detection

The Electrocardiogram signal (EKG) is characterized by five mains waves referred as P, QRS complex (three waves) and T. Each one has a specific role during the cardiac cycle and their abnormalities will lead to different diagnoses [36] or arrhythmia [37]. To date, the gold-standard of EKG analysis remains human analysis, except in specific situations such as continuous ST-segment monitoring during anesthesia of high-risk cardiac patients [38]. The PR interval is known to be linked to the autonomic nervous system [39]. Drugs

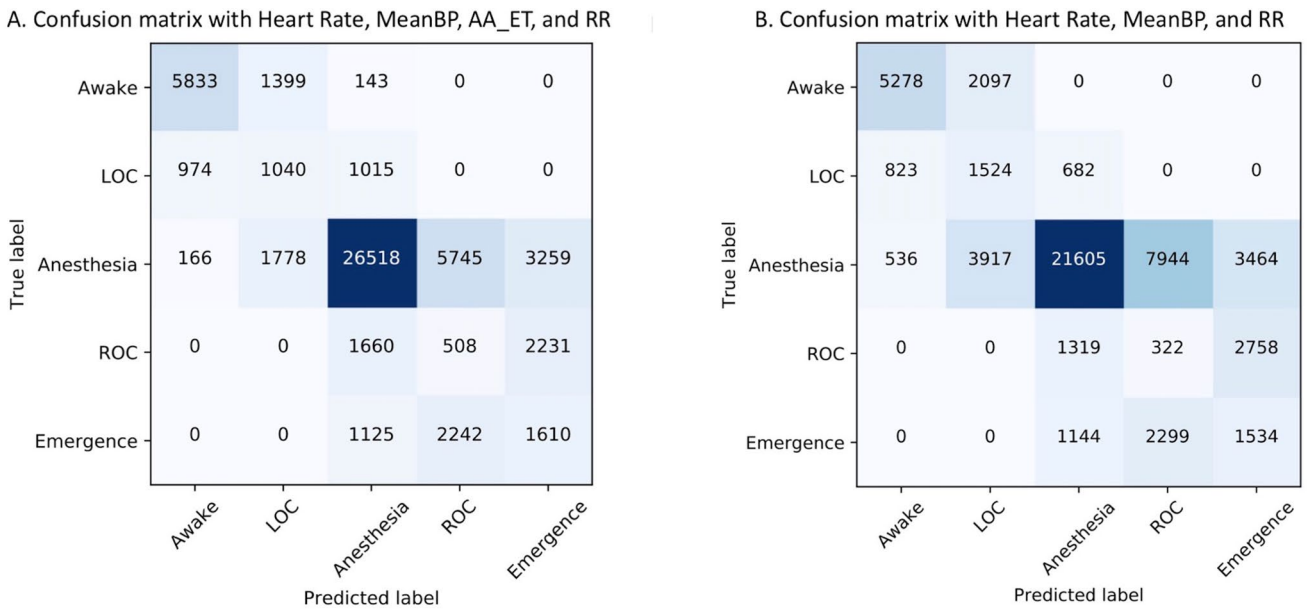

Fig. 7 Panel A: Confusion matrix when considering the four variables HR, MBP, RR and AAEt. Panel B: Confusion matrix when considering the three variables HR, MBP, RR. The rows are related to the True label and the columns are related to the predicted ones. The value in the row i column j is the number of points predict in class i while they are actually in class j. The colour ranges from white (low value) to dark blue (high value)

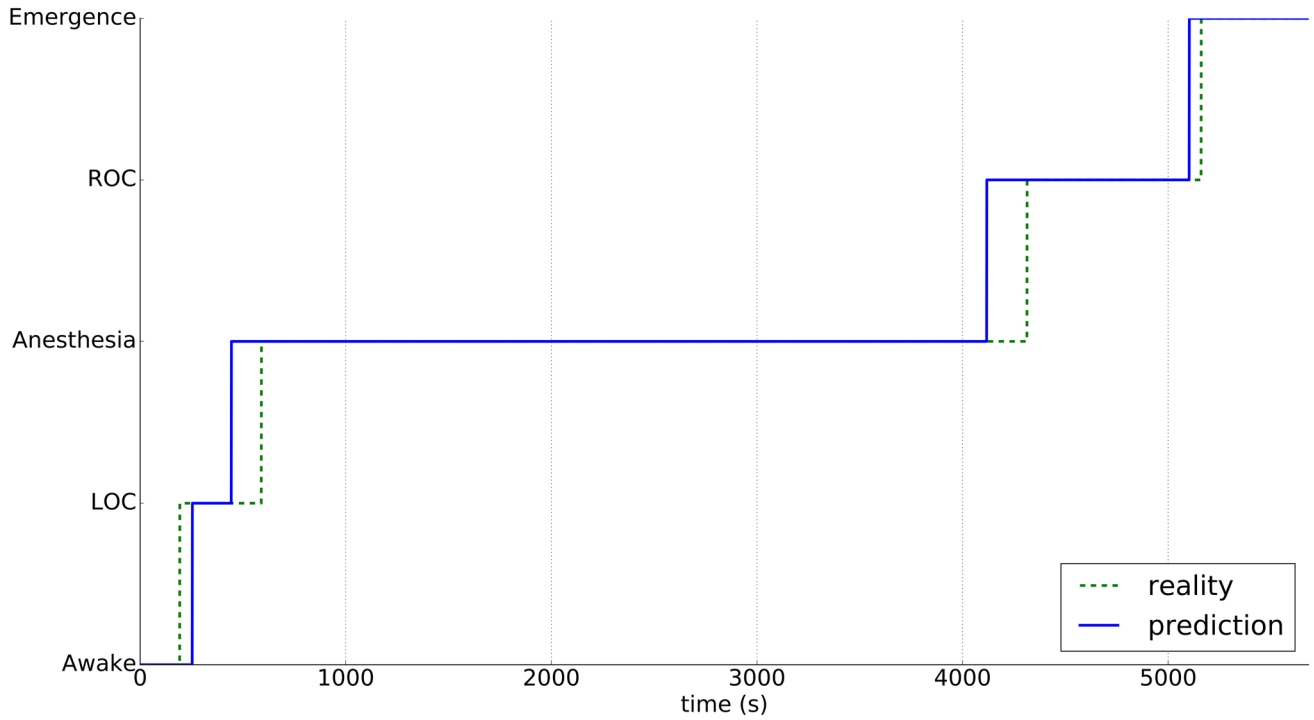

Fig. 8 In green the states of a patient during the surgery. In blue, the prediction of the HMM regarding of the physiological variables

used during anesthesia are blocking the autonomous tone, explaining in a large part the side-effects of anesthesia [40]. An automatic and real time detection of the PR interval appears potentially interesting. We present in Fig. 9 some results of an automatic detection of QRS complex with a Pan and Tompkins filtering [41].

4 Discussion

We proposed here a full protocol for high-resolution monitoring of the anesthetized patient. The three key practices in this work overlapped: the setting of sensors, the installation of all the devices and a solution to extract relevant information from the data. The confrontation with already published data proved the high quality of the recordings.

Our recording channel has proved its use with the predictive model that we developed. Despite being very preliminary, implementation of robust machine learning algorithm, allowed prediction of the DoA in our cohort with a percentage of error of only 18%. This algorithm used commonly monitored variables (HR, MBP, RR, and AAEt) and no cerebral variable to identify the DoA, which constitutes an original approach.

This constitutes the very first step on the way towards a multimodal approach of anesthesia. We believe that such a clean way to record high-resolution parameters during anesthesia will help researchers working on multiparametric approaches. For example, it has been hypothesized that cerebral autoregulation was impaired during general anesthesia [42] with a potential role in Post Operative Cognitive Dysfunction [43]. Thanks to our model, we would be able to test this hypothesis.

For a daily practice of anesthesia, an ideal DoA's monitor would provide a real-time evaluation without EEG and with a short-delay. In [28], where this protocol was used, an Hidden Markov Model (HMM) was trained in order to predict and assess states with only three physiological variables that were modified according to the level of consciousness: Heart Rate (HR), Mean Blood Pressure (MeanBP), and Respiratory Rate (RR). The Hidden Markov chain used can be defined as shown in Fig. 7. It contains the five classical states, Awake, LOC, Anesthesia, ROC and Emergence as hidden states and the probability to go from one state to another. In our model, we assume that transition only occurs between the current state and the next one. This was consistent with observations, since during the learning process, event "going back to previous state" was never identified. The interest of such a model is its ease for training and its simplicity.

Despite huge progresses in anesthesia, particularly in the field of pharmacology, assessment of the DoA remains tricky. DoA is not directly observable and can only be estimated from the knowledge gained from various variables. The most robust way for DoA assessment in clinical practice is based on online EEG analysis, particularly the frontal

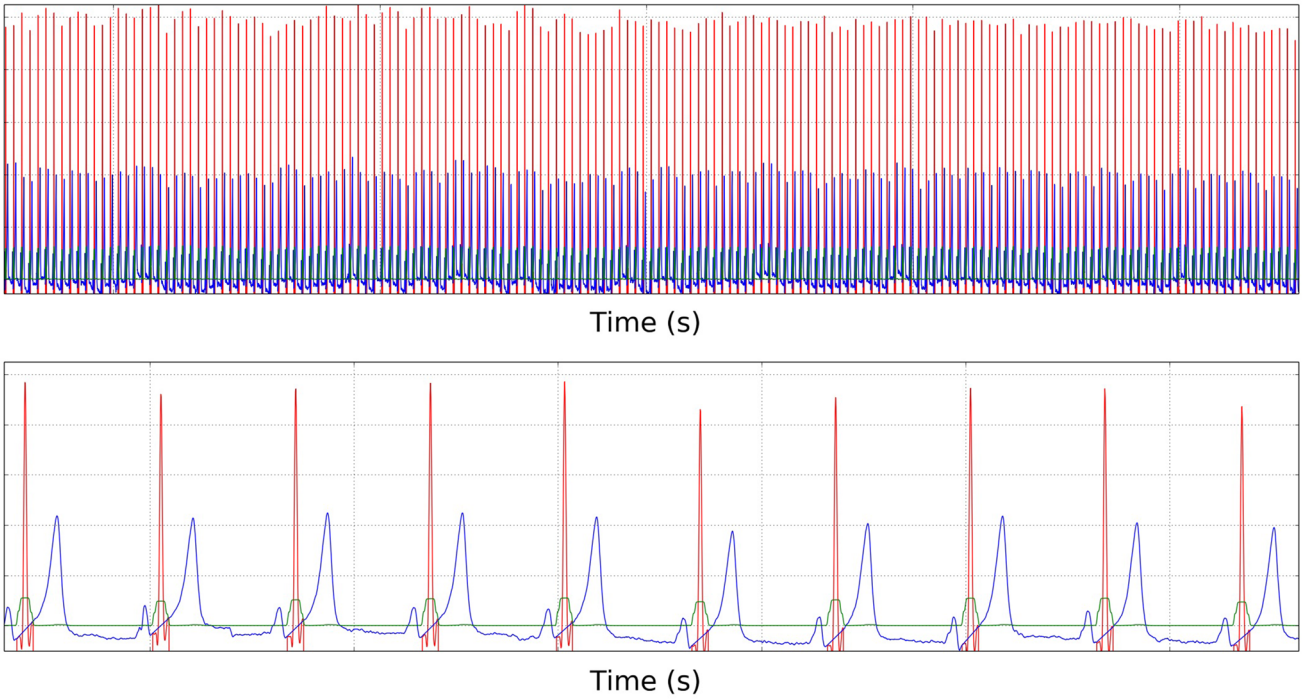

Fig. 9 Typical EKG signal where a Pan and Tompkins filtered was used. On top, a EKG signal on a long time period. In bottom a signal on a short time period. In red, the QRS complex as found by the algorithm. The green line represents the threshold value and the blue one the rest of the signal

channels [26]. For instance, Bennett et al. [44] showed that specific features of the EEG can be recognized and interpreted by anesthesiologists during a procedure. Our results are consistent with published data of spectrogram of patients under sevoflurane [45]. Indeed, extreme situations such as excessive brain activity or burst suppression state can be detected with minimal knowledge [46]. It is similar to the clinical practice of EEG outside of the anesthesia field. Some major clinical abnormalities such as status epilepticus can be detected in real-time [47]. But for other states (Loss of Consciousness (LOC), surgical anesthesia, or Recovery of Consciousness (ROC)) a precise determination is not realistic in clinical practice and remains the prerogative of research.

As a limitation of our work, we have to mention that the results presented here are drawn from a small population of 30 analyzed patients. The number of patients included has been voluntarily limited in order to carefully study the quality of the data before including more patients. It is important to note that this number of patients, somewhat small, was nevertheless sufficient to encounter the most common clinical situations of anesthesia for low-risk patients. There is no definite data to indicate which variables to include in the algorithm. To prevent overfitting, we produced the confusion matrix without taking into account the sevoflurane concentration (AAEt). Even if the results are slightly weaker without AAEt, the remaining three variables still had a good prediction. Thus, not all the information is "contained" in AAEt. However, as it improved the results, we chose to keep it in the model. Other limits of the procedure are set by sensors and more specifically by electrodes needed to record EEG signals. For example, all along surgical interventions electronic devices are continually activated and used. One can mention the electric knife to perform surgery. From this cutter, a notable number of electrical waves emanates, causing strong interferences in the recording of EEG signals (Fig. 4). These interferences resulted from a saturation of the measuring tools and not from frequencies present in the electrical waves. The use of two well-known solutions (noise reduction and outliers detection) partially resolved this problem by removing the corrupted signal [48, 49].

The fact that our first classifier already demonstrated a good predictability is very encouraging for the future. Indeed, this first model was merely a proof of concept and was based on a limited population. It is reasonable to imagine that results on a wider population will give better results. Predicting and ensuring an acceptable level of anesthesia could permit to decrease the anesthesia dose to the strict minimum required and therefore decrease the risk of complications.

Compliance with ethical standards

The study has been approved by Pr. JE BAZIN, head of the institutional ethical review board of the French society of anesthesiology (SFAR) under the number IRB 00010254-2016–2018.

References

1. Eger EI, Sonner JM. Anaesthesia defined (gentlemen, this is no humbug). Best Pract Res Clin Anaesthesiol. 2006;20:23–9.
2. Shafer S, Stanski D. Defining depth of anesthesia. Mod Anesth. 2008;182:409–23.
3. Cascella M, Viscardi D, Schiavone V, Mehrabmi-Kermani F, Muzio MR, Forte CA, et al. A 7-year retrospective multisource analysis on the incidence of anesthesia awareness with recall in cancer patients: a chance of collaboration between anesthesiologists and psycho-oncologists for awareness detection. Medicine (Baltimore). 2016;95:e2757.
4. Bruhn J, Myles PS, Sneyd R, Struys MM. Depth of anaesthesia monitoring: what's available, what's validated and what's next? Br J Anaesth. 2006;97:85–94.
5. Avidan MS, Zhang L, Burnside BA, Finkel KJ, Searleman AC, Selvidge JA, et al. Anesthesia awareness and the bispectral index. N Engl J Med. 2008;358:1097–108.
6. Kissin I. Depth of anesthesia and bispectral index monitoring. Anesth Analg. 2000;90:1114–7.
7. Whitlock EL, Villafranca AJ, Lin N, Palanca BJ, Jacobsohn E, Finkel KJ, et al. Relationship between bispectral index values and volatile anesthetic concentrations during the maintenance phase of anesthesia in the B-Unaware Trial. Anesthesiology. https://www.ncbi.nlm.nih.gov/entrez/query.fcgi?cmd=Retrieve&db=PubMed&dopt=Citation&list_uids=22037642.
8. George Mychaskiw I, Horowitz M, Sachdev V, Heath BJ. Explicit intraoperative recall at a bispectral index of 47. Anesth Analg. 2001;92:808–9.
9. Hemmerling TM, Migneault B. Falsely increased bispectral index during endoscopic shoulder surgery attributed to interferences with the endoscopic shaver device. Anesth Analg. 2002;95:1678–9.
10. Richman JS, Moorman JR. Physiological time-series analysis using approximate entropy and sample entropy. Am J Physiol-Heart Circ Physiol. 2000;278:H2039–H20492049.
11. Merry AF, Cooper JB, Soyannwo O, Wilson IH, Eichhorn JH. International standards for a safe practice of anesthesia 2010. Can J Anesth Can Anesth. 2010;57:1027–34.
12. Schneider G, Jordan D, Schwarz G, Bischoff P, Kalkman CJ, Kuppe H, et al. Monitoring depth of anesthesia utilizing a combination of electroencephalographic and standard measures. J Am Soc Anesthesiol. 2014;120:819–28.
13. Liu Q, Chen Y-F, Fan S-Z, Abbod MF, Shieh J-S. EEG signals analysis using multiscale entropy for depth of anesthesia monitoring during surgery through artificial neural networks. Comput Math Methods Med. 2015;2015:232381.
14. Sadrawi M, Fan S-Z, Abbod MF, Jen K-K, Shieh J-S. Computational depth of anesthesia via multiple vital signs based on artificial neural networks. BioMed Res Int. 2015;2015:536863.
15. Liu D, Görges M, Jenkins SA. University of Queensland vital signs dataset: development of an accessible repository of anesthesia patient monitoring data for research. Anesth Analg. 2012;114:584–9.
16. Auroy Y, Benhamou D, Bargues L, Ecoffey C, Falissard B, Mercier F, et al. Major complications of regional anesthesia in France the SOS regional anesthesia hotline service. J Am Soc Anesthesiol. 2002;97:1274–80.
17. Dutton RP. Large databases in anaesthesiology. Curr Opin Anesthesiol. 2015;28:697–702.
18. Karippacheril JG, Ho TY. Data acquisition from S/5 GE Datex anesthesia monitor using VSCapture: an open source. NET/Mono tool J Anaesthesiol Clin Pharmacol. 2013;29:423.
19. Harper AM. Autoregulation of cerebral blood flow: influence of the arterial blood pressure on the blood flow through the cerebral cortex. J Neurol Neurosurg Psychiatry. 1966;29:398–403.
20. Samuels MA. The brain–heart connection. Circulation. 2007;116:77–84.
21. Jameson LC, Sloan TB. Using EEG to monitor anesthesia drug effects during surgery. J Clin Monit Comput. 2006;20:445–72.
22. Jeleazcov C, Fechner J, Schwilden H. Electroencephalogram monitoring during anesthesia with propofol and alfentanil: the impact of second order spectral analysis. Anesth Analg. 2005;100:1365–9.
23. Robert C, Karasinski P, Arreto CD, Gaudy JF. Monitoring anesthesia using neural networks: a survey. J Clin Monit Comput. 2002;17:259–67.
24. Syroid N, Westenskow D, Bermudez J, Agutter J, Strayer D, Albert R, et al. Method and apparatus for monitoring anesthesia drug dosages, concentrations, and effects using n-dimensional representations of critical functions. Google Patents; 2007.
25. Berthomier C, Brandewinder M, Berthomier P, Mattout J, Sagaspe P, Philip P, et al. Analyse automatique du sommeil à partir d'une unique dérivation EEG: validation chez des patients ayant des troubles cognitifs légers. Médecine Sommeil. 2016;13:30–1.
26. Purdon PL, Pierce ET, Mukamel EA, Prerau MJ, Walsh JL, Wong KFK, et al. Electroencephalogram signatures of loss and recovery of consciousness from propofol. Proc Natl Acad Sci. 2013;110:E1142–E1151151.
27. Bartlett MS. Smoothing periodograms from time series with continuous spectra. Nature. 1948;161:686–7.
28. Humbert P, Dubost C, Audiffren J, Oudre L. Learning from an expert in anesthesia. Workshop Mach Learn Health Neural Inf Process Syst. 2016.
29. Adeli H, Zhou Z, Dadmehr N. Analysis of EEG records in an epileptic patient using wavelet transform. J Neurosci Methods. 2003;123:69–87.
30. Subasi A. EEG signal classification using wavelet feature extraction and a mixture of expert model. Expert Syst Appl. 2007;32:1084–93.
31. Zikov T, Bibian S, Dumont GA, Huzmezan M, Ries CR. Quantifying cortical activity during general anesthesia using wavelet analysis. IEEE Trans Biomed Eng. 2006;53:617–32.
32. Anderson CW, Stolz EA, Shamsunder S. Multivariate autoregressive models for classification of spontaneous electroencephalographic signals during mental tasks. IEEE Trans Biomed Eng. 1998;45:277–86.
33. Laitio RM, Kaskinoro K, Särkelä MO, Kaisti KK, Salmi E, Maksimow A, et al. Bispectral index, entropy, and quantitative electroencephalogram during single-agent xenon anesthesia. J Am Soc Anesthesiol. 2008;108:63–70.
34. Wang H, Song M. Ckmeans.1d.dp: optimal k-means clustering in one dimension by dynamic programming. R J. 2011;3:29–33.
35. Dubost C, Humbert P, Oudre L, Buffat S, Ould-Ahmed M. Longitudinal individual follow-up of physiological variables during general anesthesia: development of a mathematical signature of general anesthesia. Eur J Anaesthesiol. 2017;34:28.
36. Thakor NV, Zhu Y-S. Applications of adaptive filtering to ECG analysis: noise cancellation and arrhythmia detection. IEEE Trans Biomed Eng. 1991;38:785–94.
37. Taillefer R, DePuey EG, Udelson JE, Beller GA, Latour Y, Reeves F. Comparative diagnostic accuracy of Tl-201 and Tc-99m

sestamibi SPECT imaging (perfusion and ECG-gated SPECT) in detecting coronary artery disease in women. J Am Coll Cardiol. 1997;29:69–77.
38. Landesberg G, Mosseri M, Wolf Y, Vesselov Y, Weissman C. Perioperative myocardial ischemia and infarction identification by continuous 12-lead electrocardiogram with online ST-segment monitoring. J Am Soc Anesthesiol. 2002;96:264–70.
39. Shouldice R, Heneghan C, Nolan P, Nolan P. PR and PP ECG intervals as indicators of autonomic nervous innervation of the cardiac sinoatrial and atrioventricular nodes. First Int IEEE EMBS Conf Neural Eng. 2003;2003:261–4.
40. Gelman S, Mushlin PS. Catecholamine-induced changes in the splanchnic circulation affecting systemic hemodynamics. J Am Soc Anesthesiol. 2004;100:434–9.
41. Pan J, Tompkins WJ. A real-time QRS detection algorithm. IEEE Trans Biomed Eng. 1985;3:230–6.
42. McCulloch TJ, Visco E, Lam AM. Graded hypercapnia and cerebral autoregulation during sevoflurane or propofol anesthesia. J Am Soc Anesthesiol. 2000;93:1205–9.
43. Paredes S, Cortínez L, Contreras V, Silbert B. Post-operative cognitive dysfunction at 3 months in adults after non-cardiac surgery: a qualitative systematic review. Acta Anaesthesiol Scand. 2016;60:1043–58.
44. Bennett C, Voss LJ, Barnard JP, Sleigh JW. Practical use of the raw electroencephalogram waveform during general anesthesia: the art and science. Anesth Analg. 2009;109:539–50.
45. Purdon PL, Sampson A, Pavone KJ, Brown EN. Clinical electroencephalography for anesthesiologistspart I: background and basic signatures. J Am Soc Anesthesiol. 2015;123:937–60.
46. Bottros MM, Palanca BJA, Mashour GA, Patel A, Butler C, Taylor A, et al. Estimation of the bispectral index by anesthesiologists an inverse turing test. J Am Soc Anesthesiol. 2011;114:1093–101.
47. Privitera M, Hoffman M, Moore JL, Jester D. EEG detection of nontonic-clonic status epilepticus in patients with altered consciousness. Epilepsy Res. 1994;18:155–66.
48. Ott HW, Ott HW. Noise reduction techniques in electronic systems. New York: Wiley; 1988.
49. Rousseeuw PJ, Leroy AM. Robust regression and outlier detection. New York: Wiley; 2005.